Journal of Alloys and Compounds 515 (2012) 16–19

Contents lists available at SciVerse ScienceDirect

Journal of Alloys and Compounds

journal homepage: www.elsevier.com/locate/jallcom

Letter

Multiwavelength excited white-emitting phosphor Dy^{3+}-activated $Ba_3Bi(PO_4)_3$

Qingbo Liu [a,b], Yufeng Liu [a,*], Zhiping Yang [a], Yue Han [a], Xu Li [a], Guangsheng Fu [a]

[a] College of Physics Science and Technology, Hebei University, Baoding 071002, China
[b] Department of Physics, Baoding University, Baoding 071002, China

ARTICLE INFO

Article history:
Received 17 September 2011
Received in revised form
22 November 2011
Accepted 23 November 2011
Available online 2 December 2011

Keywords:
Phosphors
Solid state reactions
Optical properties
Luminescence

ABSTRACT

Dy^{3+}-activated $Ba_3Bi(PO_4)_3$ multiwavelength excited warm white emitting phosphors were synthesized via a solid state reaction at 1250 °C. The structure and photoluminescence characteristics were investigated by X-ray powder diffraction (XRD) and fluorescent spectrophotometry, respectively. The excitation spectra included some bands located at 348.2, 362.6, 386.8 and 452.4 nm which match the radiations of near-UV or blue light-emitting diodes chip well. Upon excitation either of near-UV or blue even green light, the intense blue and yellow emissions with 481.6 (487) and 575 nm peaks can be observed, which is ascribed to the $^4F_{9/2}$–$^6H_{15/2}$, $^4F_{9/2}$–$^6H_{13/2}$ transitions of Dy^{3+} ions. The chromaticity coordinates ($x = 0.322$, $y = 0.381$) of the as-obtained phosphor is very close to the "ideal white" ($x = 0.333$, $y = 0.333$) in chromaticity diagram. All these characteristics suggest that Dy^{3+}-doped $Ba_3Bi(PO_4)_3$ wavelength-conversion material to be suitable candidate warm white component for phosphor converted white light-emitting diodes.

1. Introduction

Recently, trivalent dysprosium ions (Dy^{3+}) doped phosphors have been extensively studied due to the potential applications in white light emission, because of its intense blue (484 nm, $^4F_{9/2}$–$^6H_{15/2}$) and yellow (575 nm, $^4F_{9/2}$–$^6H_{13/2}$) emissions [1]. However, In different hosts, the ratio of the two dominant Dy^{3+} emission bands arising from the transitions $^4F_{9/2}$–$^6H_{15/2}$ (blue) and $^4F_{9/2}$–$^6H_{13/2}$ (yellow) is different, because the yellow emission is strongly influenced by the chemical environment surrounding Dy^{3+} due to $\Delta J = 2$ ($^4F_{9/2}$–$^6H_{13/2}$), while the blue emission ($^4F_{9/2}$–$^6H_{15/2}$) is relatively invariable. Therefore, the color tone of Dy^{3+}-doped phosphors can be modified by changing the relative intensity of the yellow light through crystal field engineering. At present, There are many hosts that can be activated by Dy^{3+} ions, such as borates [2–4], phosphates [5–8], aluminates [9,10], silicates [11–13], vanadates [14–16], and molybdates [1]. Among these phosphors investigated, phosphates are good candidates due to their low synthetic temperatures, stabilities, and low costs.

In recent, Zhang and co-workers reported the red-emitting phosphor $Ba_3Bi_{1-x}(PO_4)_3$:xEu^{3+} for w-LED [17]. They found that the integral intensity of the emission spectrum excited at 393 nm is about twice as strong as that of Y_2O_3:Eu^{3+} commercial red phosphor. So, the $Ba_3Bi(PO_4)_3$ compound is a good type of promising host materials for rare earth ions doped phosphor. However, To the best of our knowledge, the photoluminescence (PL) properties of $Ba_3Bi(PO_4)_3$:Dy^{3+} phosphors have not been reported yet. In this article, to find a warm white phosphor for solid state light, a series of $Ba_3Bi(PO_4)_3$:xDy^{3+} ($0.005 \le x \le 0.15$) phosphors was synthesized, and their PL properties were investigated.

2. Experimental

Powder samples $Ba_3Bi(PO_4)_3$:Dy^{3+} were prepared by solid-state reaction. The starting materials included $BaCO_3$ (A.R.), Bi_2O_3 (A.R.), $NH_4H_2PO_4$ (A.R.), and Dy_2O_3 (99.99%). Stoichiometric amounts of the starting reagents were thoroughly mixed and ground together by an agate mortar. An excess (2%) of $NH_4H_2PO_4$ was used to compensate for the evaporation of $NH_4H_2PO_4$ at a high temperature in solid-state reactions. In order to obtain the target compound with pure phase, two firing steps were necessary. The mixture was firstly heated at 500 °C for 5 h in a covered alumina crucible, then reground thoroughly after cooled down to the room temperature. The second firing was conducted at 1250 °C for 3 h. Finally, the samples are ground into powder for characterizations.

The powder sample was characterized by X-ray diffraction (XRD) in a Bruker AXS D8 advanced automatic diffractometer (Bruker Co., German) with Ni-filtered Cu Kα1 radiation ($\lambda = 1.5405$ Å). A scan rate of 0.02°/s was applied to record the patterns in the 2θ range 10–90°. Photoluminescence (PL) excitation and emissions spectra were collected in a fluorescence spectrophotometer (Hitachi F-4600). The chromaticity data were taken by using the PMS-80 spectra analysis system. All the measurements were conducted at room temperature.

3. Results and discussion

The $Ba_3Bi(PO_4)_3$ compound has the structural type of eulytine, and Bi^{3+} ion occupies a distorted octahedron of oxygen ions due to three short and three long Bi–O distances, according to Ref. [18]. Therefore, we can predict that Bi^{3+} ions occupy noninversion centrosymmetric sites. We also assume that Bi^{3+} ions are replaced by

* Corresponding author. Tel.: +86 312 5079423; fax: +86 312 5011174.
E-mail address: liuyufeng4@126.com (Y. Liu).

0925-8388/$ – see front matter © 2011 Elsevier B.V. All rights reserved.
doi:10.1016/j.jallcom.2011.11.114

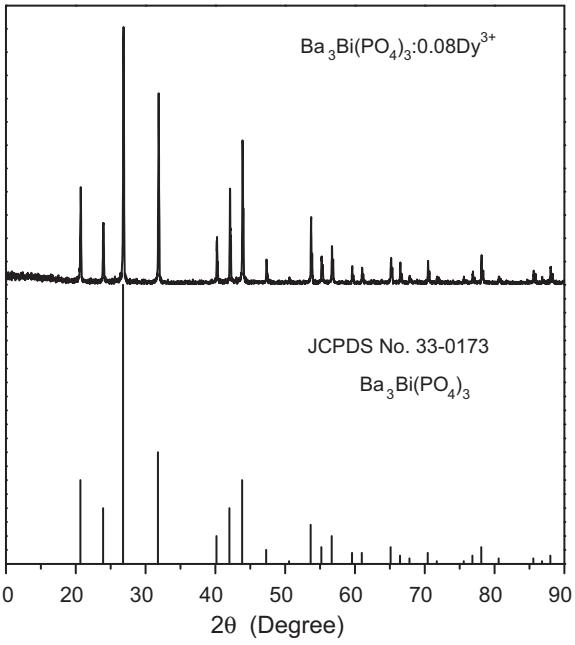

Fig. 1. The XRD patterns of typical sample $Ba_3Bi(PO_4)_3$:0.08Dy^{3+} and the standard data JCPDS card No. 33-0173 of $Ba_3Bi(PO_4)_3$.

Dy^{3+} ions in $Ba_3Bi(PO_4)_3$:Dy^{3+} because they have the same valence and ionic radii [19]. The body colors of as-obtained phosphor powders are white. Fig. 1 shows the X-ray powder diffraction patterns of typical sample $Ba_3Bi(PO_4)_3$:0.08Dy^{3+} phosphor, and all the diffraction peaks can be indexed to pure cubic-structured $Ba_3Bi(PO_4)_3$ (JCPDS card no. 33-0173). No obvious impurity phase was detected when Dy^{3+} was doped into the host lattice. These results indicated that Dy^{3+} ions were undoubtedly doped into and entered the $Ba_3Bi(PO_4)_3$ crystal lattice.

Fig. 2 displays the excitation spectra of $Ba_3Bi(PO_4)_3$:xDy^{3+} phosphors with various x values. When the x value changed from 0.005 to 0.15, the excitation spectra were similar except that the intensity of excitation peaks. Under monitoring at 575 nm corresponding to $^4F_{9/2}$–$^6H_{13/2}$ emission of Dy^{3+} ions, the spectra were made up of a series of bands. The peaks located at 323.2, 348.2, 362.6, 386.8, 424.2, 452.4 and 467.6 (472.6) nm belong to the intrinsic f–f transitions of Dy^{3+} from the ground state $^6H_{15/2}$ to the excited state $^4L_{19/2}$, $^6P_{7/2}$, $^6P_{5/2}$, $^4I_{13/2}$, $^4G_{11/2}$, $^4I_{15/2}$ and $^4F_{9/2}$, respectively [1]. Of these excitation lines, the intensities of the 348.2, 362.6, 386.8 and 452.4 nm excitation peaks are much stronger than the others, which indicates that near-UV and blue LEDs are efficient pumping sources in obtaining Dy^{3+} emissions.

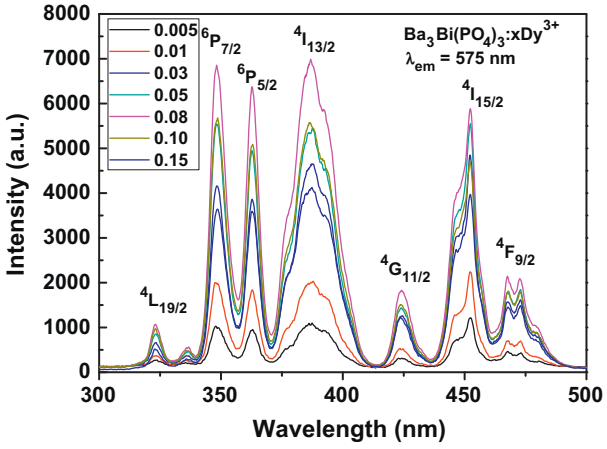

Fig. 2. The excitation spectra of the samples $Ba_3Bi(PO_4)_3$:xDy^{3+} with various x values (monitoring wavelength λ_{em} = 575 nm).

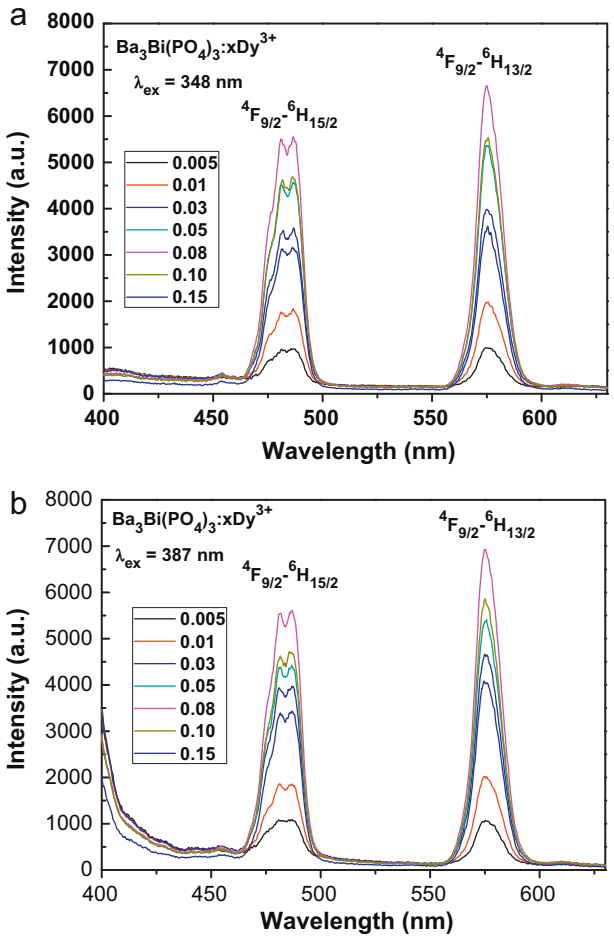

Fig. 3. The fluorescence emission spectra of $Ba_3Bi(PO_4)_3$:xDy^{3+} phosphors with different x values under various excitation wavelength λ_{ex} = 348 nm (a) and λ_{ex} = 387 nm (b).

Fig. 3 shows the emission spectra of $Ba_3Bi(PO_4)_3$:xDy^{3+} phosphors excited by 348 nm and 387 nm UV light. It can be seen from the emission spectra that all the profiles of the emission spectra of $Ba_3Bi(PO_4)_3$:Dy^{3+} are similar, and there are two dominating emissions at 481.6 (487) and 575 nm, corresponding to $^4F_{9/2}$–$^6H_{15/2}$, $^4F_{9/2}$–$^6H_{13/2}$ transitions, respectively. The $^4F_{9/2}$–$^6H_{13/2}$ transition belongs to a forced electric dipole transition, which is allowed only in the case that the Dy^{3+} ions are located at the local sites with non-inversion center symmetry. In $Ba_3Bi(PO_4)_3$:Dy^{3+}, from the emission spectra, the yellow emission ($^4F_{9/2}$–$^6H_{13/2}$) is stronger than the blue emission ($^4F_{9/2}$–$^6H_{15/2}$), indicating that Dy^{3+} is located in more non-centrosymmetric position in the $Ba_3Bi(PO_4)_3$ matrix, which agrees with the conclusion of the structural analysis.

The emission spectra of $Ba_3Bi(PO_4)_3$:xDy^{3+} phosphors under 348.2, 362.6, 386.8 and 452.4 nm excitation show roughly the same position of emission peaks, except for the intensity (not shown). The emission intensity corresponding to the 348 and 387 nm excitation are higher than that of other wavelengths because of the relatively higher absorption at these wavelengths.

In order to obtain the best doping concentration of Dy^{3+}, a series of $Ba_3Bi(PO_4)_3$:xDy^{3+} ($0.005 \le x \le 0.15$) phosphors was prepared. The change of emission intensity of $Ba_3Bi(PO_4)_3$:xDy^{3+} as a function of Dy^{3+} concentration (x = 0.005, 0.01, 0.03, 0.05, 0.08, 0.10, 0.15) is shown in Fig. 4. It can be seen from Fig. 4 that all the profiles of the

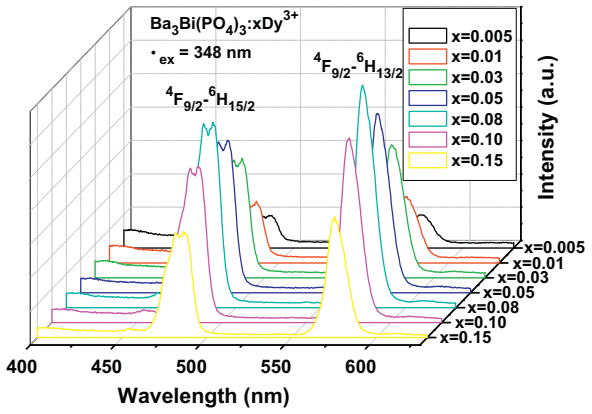

Fig. 4. The emission intensity of $Ba_3Bi(PO_4)_3$:xDy^{3+} as a function of Dy^{3+} concentration.

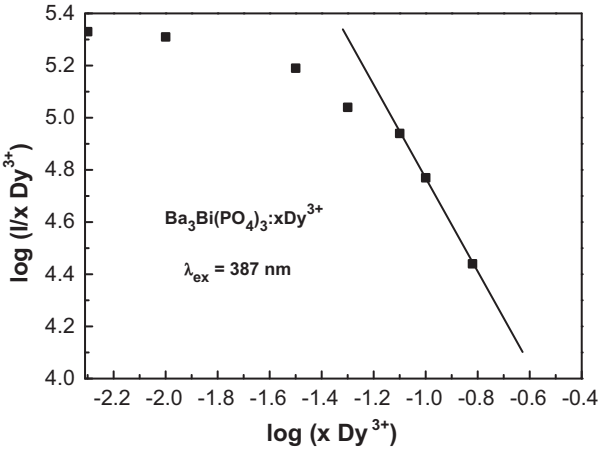

Fig. 5. Log plot for the emission intensity at 575 nm per activator ions (Dy^{3+}) as a function of the activator concentration (λ_{ex} = 387 nm).

emission spectra of different content of Dy^{3+} doped $Ba_3Bi(PO_4)_3$ are similar, and the integrated emission intensity ratios of $^4F_{9/2}$–$^6H_{13/2}$ to $^4F_{9/2}$–$^6H_{15/2}$ for all the samples were calculated to be about a constant value 1.2, which demonstrates that the Dy^{3+} introduction does not result in an obvious change of the crystal structure and crystal field environment surrounding the Dy^{3+} ions even at such a high doping level as 15 mol%.

From Fig. 4, it also can be seen that as the Dy^{3+} concentration increases, the emission intensity increases, and it maximizes at about $x = 0.08$, which is taken as the critical concentration. Lower doping concentrations lead to weak luminescence of the Dy^{3+} emission. Beyond the critical concentration, the intensity gradually decreases as the Dy^{3+} concentration increases because of the concentration quenching. The concentration quenching is mainly caused by the nonradiative energy transfer among Dy^{3+} ions, which usually occurs as a result of an exchange interaction, radiation reabsorption, or a multipole–multipole interaction [20].

It is necessary to obtain the critical distance (R_c) that is the critical separation between the donor (activator) and acceptor (quenching site). According to the report of Blasse [21], if the activator is introduced solely on Z ion sites, where x_c is the critical concentration of the activator ion, N is the number of Z ions in the unit cell, and V is the volume of the unit cell, then there is on the average one activator ion per V/x_cN. The critical transfer distance (R_c) is approximately equal to twice the radius of a sphere with this volume

$$R_c \approx 2\left[\frac{3V}{4\pi x_c N}\right]^{1/3} \quad (1)$$

for the $Ba_3Bi(PO_4)_3$ host, when $N = 4$ ($Z = 1$), $x_c = 0.08$, and $V = 1158.8$ Å^3 [18], the obtained R_c value is 19 Å. According to Ref. [22], nonradiative energy transfer in the luminescence of oxidic phosphors is based on resonance transfer by electric multipole–multipole interaction or exchange interaction. The situation in Dy^{3+} compounds can be characterized as follows: [23] If the Dy^{3+}–Dy^{3+} distance is larger than 5 Å, the exchange interaction becomes ineffective, and only a multipolar interaction is important; if the Dy^{3+}–Dy^{3+} distance is shorter than 5 Å, the exchange interaction becomes effective. As the R_c of Dy^{3+}–Dy^{3+} for $Ba_3Bi(PO_4)_3$:Dy^{3+} phosphor is calculated to be 19 Å, the multipolar interaction is the major mechanism of concentration quenching of Dy^{3+} in the $Ba_3Bi(PO_4)_3$:Dy^{3+} phosphor.

When the electric multipolar interaction is involved in the energy transfer, there are several types of interactions, such as dipole–dipole (d–d), dipole–quadrupole (d–q), quadrupole–quadrupole (q–q) interactions, and so on. Thus, there is a need to elucidate which type of interaction is involved in the energy transfer. According to the theory of Dexter, the relation between luminescent intensity (I) and the activator concentration (x) can be expressed by an equation, the modified equation is as follows [24]:

$$I \propto \frac{1+A}{\gamma}\left[\frac{3\Gamma(1+s/3)}{\alpha^{1-s}}\right] \quad (\alpha \geq 1) \quad (2)$$

where $\alpha = x[(1+A)X_0/\gamma]^{3/s}\Gamma(1-s/3) \propto x$, x is the activator concentration, s is the series of electric multipolar (there are four different quenching mechanisms, i.e. exchange interactions, d–d, d–q and q–q when the values of s are 3, 6, 8 and 10, respectively), γ is the intrinsic transition probability of activator, A and X_0 are the constants.

From the slope of Eq. (2), the electric multipolar character (s) can be obtained by the slope ($-s/3$) of the plot $\log(I/x)$ vs $\log x$. Fig. 5 shows the relation between $\log(I/x)$ and $\log x$ in $Ba_3Bi(PO_4)_3$:Dy^{3+} phosphor (λ_{ex} = 387 nm). Since the critical concentration of Dy^{3+} has been determined as 8 mol%, the dependence of the emission intensity of the $Ba_3Bi(PO_4)_3$:Dy^{3+} phosphor excited at 387 nm on the doped-Dy^{3+} concentration which is not less than the critical concentration (8 mol%) is determined (see Fig. 5). It can be seen from Fig. 5, that the dependence of $\log(I/x)$ on $\log x$ is linear and the slope is −2.03. Thus, the value of s can be calculated as 6.09 (very close to the theoretical value 6 for the electric d–d interaction), which means that the d–d interaction is the main mechanism for the concentration quenching of $^4F_{9/2}$–$^6H_{13/2}$ transition of Dy^{3+} in the $Ba_3Bi(PO_4)_3$:Dy^{3+} phosphor. Considering the energy match rule

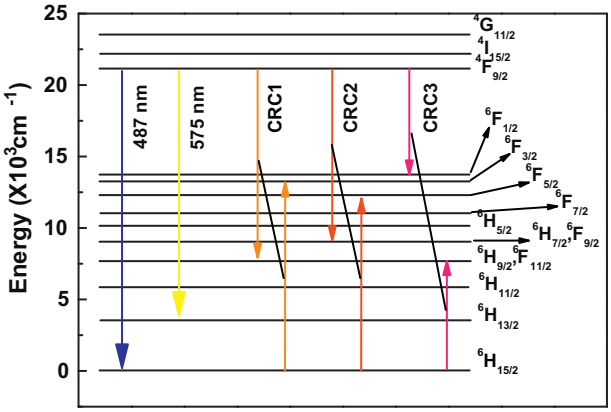

Fig. 6. Energy level scheme of Dy^{3+} represents the mechanisms for different observed emissions and possible cross-relaxation processes.

Table 1
CIE chromaticity coordinates values of $Ba_3Bi(PO_4)_3$:xDy^{3+} system under various excitation wavelength λ_{ex} = 348 nm and λ_{ex} = 387 nm.

$Ba_3Bi(PO_4)_3$:xDy^{3+}	x = 0.005	x = 0.01	x = 0.03	x = 0.05	x = 0.08	x = 0.10	x = 0.15
λ_{ex} = 348 nm							
(x)	0.318	0.320	0.323	0.325	0.322	0.324	0.326
(y)	0.383	0.382	0.379	0.381	0.381	0.379	0.378
λ_{ex} = 387 nm							
(x)	0.317	0.319	0.321	0.321	0.321	0.324	0.327
(y)	0.379	0.381	0.380	0.379	0.380	0.383	0.382

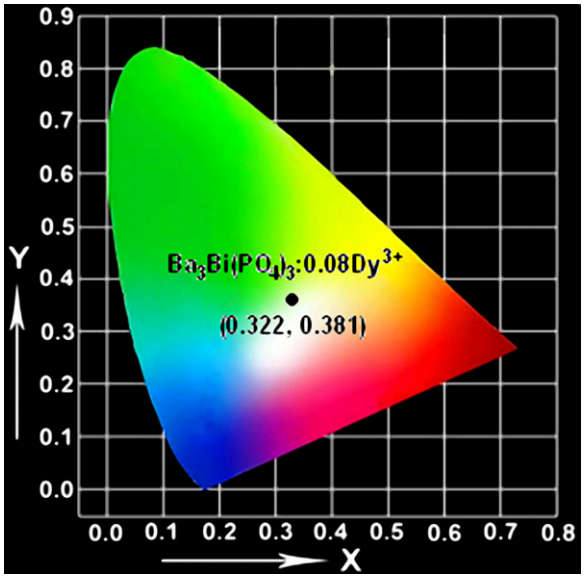

Fig. 7. The CIE chromaticity coordinate for the prepared typical samples $Ba_3Bi(PO_4)_3$:$0.08Dy^{3+}$ under the excitation wavelength of 348 nm.

[1], three possible cross-relaxation channels (CRC) among Dy^{3+} are shown in Fig. 6, denoted as CRC1, CRC2 and CRC3. The Dy^{3+} ions at $^4F_{9/2}$ level can be de-excited to ($^6F_{9/2}$/$^6H_{7/2}$), ($^6H_{9/2}$/$^6F_{11/2}$) or $^6F_{1/2}$ level via these three cross-relaxation processes, in the mean while the ground state Dy^{3+} ions accepting the energies from the Dy^{3+} at $^4F_{9/2}$ level will arrive at $^6F_{3/2}$, $^6F_{5/2}$ and ($^6H_{9/2}$/$^6F_{11/2}$) level. Finally, all the Dy^{3+} ions involved in CRC1, CRC2 and CRC3 processes will get in their ground states, thus the luminescence related to $^4F_{9/2}$ level are quenched.

Color coordinates are one of the important factors for evaluating phosphors' performance. It is a well known fact that the color coordinates are the same if the spectra profiles are identical. In such case, the color coordinates for the sample doped with 8 mol% Dy^{3+} were calculated using the intensity-calibrated emission spectra data and the chromatic standard issued by the Commission International de l'Eclairage in 1931 (CIE 1931). The CIE chromaticity coordinate for the prepared samples $Ba_3Bi(PO_4)_3$:$0.08Dy^{3+}$ are shown in Fig. 7 with the dot symbols (λ_{ex} = 348 nm). It can be seen that the color coordinates of $Ba_3Bi(PO_4)_3$:$0.08Dy^{3+}$ for full emissions are x = 0.322, y = 0.381, which is depicted by warm white very near to "ideal white" in chromaticity diagram. In order to further improve the CIE colorcoordinates and achieve good quality white light emission, some other rare earth dopants, emitting blue may need to be introduced into this phosphor system.

The CIE chromaticity coordinates values measured from $Ba_3Bi(PO_4)_3$:xDy^{3+} system under various excitation wavelength λ_{ex} = 348 nm and λ_{ex} = 387 nm are listed in Table 1. From Table 1, it can be seen that CIE chromaticity coordinates values are stable basically with increasing x, and the chromaticity coordinates of almost all the prepared samples locate in white light region in CIE-1931 chromaticity diagram.

4. Conclusions

The novel warm white phosphor $Ba_3Bi(PO_4)_3$:xDy^{3+} with various Dy^{3+} concentrations was synthesized by the conventional solid-state reaction at 1250 °C in air. The crystal structure of the phosphor was characterized by XRD. The photoluminescence properties of $Ba_3Bi(PO_4)_3$:xDy^{3+} were investigated. The optimized phosphor with the composition of $Ba_3Bi(PO_4)_3$:$0.08Dy^{3+}$ presents the several excitation bands from 300 to 500 nm, and exhibits very good luminescence properties. Under the ultraviolet excitation of 348 and 387 nm, the phosphor presented warm white luminescence with dominating emissions at 481.6 (487) and 575 nm, corresponding to $^4F_{9/2}$–$^6H_{15/2}$, $^4F_{9/2}$–$^6H_{13/2}$ transitions, respectively. The chromatic properties of the typical sample $Ba_3Bi(PO_4)_3$:$0.08Dy^{3+}$ phosphor have been found to have chromaticity coordinates of x = 0.322 and y = 0.381 under the excitation wavelength λ_{ex} = 348 nm.

Acknowledgments

This work was financially supported by the National Natural Science Foundation of China (Grant no. 50902042) and the Science and Technology Project of Hebei Province (Grant no. F2009000217).

References

[1] L.H. Cheng, X.P. Li, J.S. Sun, H.Y. Zhong, Y. Tian, J. Wan, W.L. Lu, Y.F. Zheng, T.T. Yu, L.B. Huang, H.Q. Yu, B.J. Chen, Physica B 405 (2010) 4457.
[2] P.L. Li, Z.P. Yang, Z.J. Wang, Q.L. Guo, Mater. Lett. 62 (2008) 1455.
[3] R. Zhang, X. Wang, J. Alloys Compd. 509 (2011) 1197.
[4] B. Vengala Rao, S. Buddhudu, Spectrochim. Acta A 71 (2008) 951.
[5] Z.L. Xiu, Z.S. Yang, M.K. Lv, S.W. Liu, H.P. Zhang, G.J. Zhou, Opt. Mater. 29 (2006) 431.
[6] H. Lai, A. Bao, Y.M. Yang, W.W. Xu, Y.C. Tao, H. Yang, J. Lumin. 128 (2008) 521.
[7] K.N. Shinde, S.J. Dhoble, A. Kumar, Physica B 406 (2011) 94.
[8] K.N. Shinde, S.J. Dhoble, A. Kumar, J. Lumin. 131 (2011) 931.
[9] P. Huang, C.E. Cui, S. Wang, Opt. Mater. 32 (2009) 184.
[10] K. Pavani, J.S. Kumar, T. Sasikala, B.C. Jamalaiah, H.J. Seo, L.R. Moorthy, Mater. Chem. Phys. 129 (2011) 292.
[11] B. Liu, L.J. Kong, C.S. Shi, J. Lumin. 121 (2007) 122.
[12] Y. Fang, W.D. Zhuang, Y.S. Hu, X.Y. Ye, X.W. Huang, J. Alloys Compd. 455 (2008) 420.
[13] L.L. Martin, P. Haro-González, I.R. Martín, Opt. Mater. 33 (2011) 738.
[14] S.D. Han, S.P. Khatkar, V.B. Taxak, G. Sharma, D. Kumar, Mater. Sci. Eng. B 129 (2006) 126.
[15] A. Bao, H. Yang, C.Y. Tao, Y. Zhang, L.L. Han, J. Lumin. 128 (2008) 60.
[16] B. Yan, X.Q. Su, Mater. Lett. 61 (2007) 482.
[17] J. Zhang, Y.H. Wang, Electrochem. Solid-State Lett. 13 (2010) J35.
[18] E.H. Arbib, B. Elouadi, J.P. Chaminade, J. Darriet, Mater. Res. Bull. 35 (2000) 761.
[19] T. Tsuboi, H.J. Seo, B.K. Moon, J.H. Kim, Physica B 270 (1999) 45.
[20] D.L. Dexter, J. Chem. Phys. 21 (1953) 836.
[21] G. Blasse, J. Solid State Chem. 62 (1986) 207.
[22] G. Blasse, Philips Res. Rep. 24 (1969) 131.
[23] G. Blasse, B.C. Grabmarier, Luminescent Materials, Springer-Verlag, Berlin, 1994, p. 99.
[24] D.L. Dexter, J.H. Schulman, J. Chem. Phys. 22 (1954) 1063.